THE JOURNAL OF PHYSICAL CHEMISTRY A

Article

pubs.acs.org/JPCA

Jet-Cooled Fluorescence Spectroscopy of a Natural Product: Anethole

Victoria P. Barber and Josh J. Newby*

Department of Chemistry and Biochemistry, Swarthmore College, 500 College Avenue, Swarthmore, Pennsylvania 19081, United States

Supporting Information

ABSTRACT: The jet-cooled fluorescence spectroscopy of the natural product molecule anethole ((*E*)-1-methoxy-4-(1-propenyl)benzene) has been studied. Single vibronic level fluorescence spectroscopy was used to verify the existence of two rotamers, syn and anti, with electronic origins at 32 889 and 32 958 cm^{-1}, respectively. The excitation and emission spectra show characteristics similar to those of styrene and styrene derivatives, including C_s symmetry and low amplitude motions of the propenyl (vinyl) group. As in styrene, the low amplitude modes show substantial Duschinsky mixing. Interestingly, the methoxy group shows very little activity in the spectroscopy of anethole but is found to influence the activity of the propenyl group. This activity is easily observed in the Franck−Condon activity of the propenyl-bending mode. Differences are explained using simple molecular orbital arguments. The observed torsional structure was modeled and compared to ab initio calculations, allowing us to determine a barrier to internal rotation of 623 cm^{-1} for the propenyl group, in agreement with similar molecules. Calculated potential energy surfaces (using density functional theory) were used to construct a more complete representation of the torsion surface of anethole, incorporating the torsions of both substituents. Several anomalous features of the excitation spectra were assigned to van der Waals clusters of anethole with water. The assignments and analyses presented here are also consistent with density function calculations.

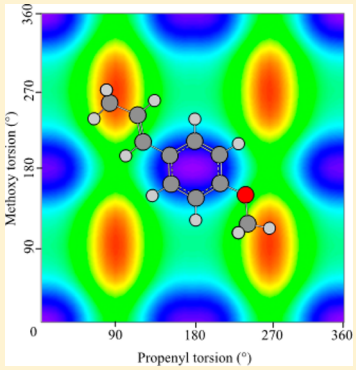

I. INTRODUCTION

A. Natural Product Molecules. Plants have been adapting to their environments for countless years. Though many think about organism level adaptations, we can also observe adaptation at the molecular level. Plant species create a wide variety of molecules that serve specific purposes. Phenylpropanoids are a family of compounds that provide protection from ultraviolet radiation, herbivores and pathogens, or attract pollinators.[1] Within this family is the phenylpropene subgroup, which includes many molecules that are commonly attributed to scents or flavors of essential oils. Anethole ((*E*)-1-methoxy-4-(1-propenyl)-benzene) is a phenylpropene that is a component of several essential oils.

Anethole is commonly used as a flavoring agent, with the distinct flavor commonly noted in anise, fennel, or licorice. In several species, this molecule is generated to help attract pollinators but can also serve as an antimicrobial when found in higher concentrations.[1,2] Interestingly, plants synthesize the *E* isomer almost exclusively. Anise seed oil, for example, is made up of 94% (*E*)-anethole and less than 1% (*Z*)-anethole.[3] Although the *E* isomer is often used as a flavor or scent agent, the *Z* isomer is not, as it has a less pleasant aroma. It is most fascinating that something as simple as an *E*/*Z* isomerization can lead to such a change in sensory input. Because the *Z* isomer is more sterically hindered, we predict that there will be additional geometric difference between the two isomers. Our group is interested in the geometric and dynamical differences that occur in flavor molecule isomers. Spectroscopic analysis will allow us to build a finer description of these molecules in the gas phase that may be useful in understanding how they affect sensory input. The current study will focus on the *E* isomer of anethole.

B. Flexible Molecules. Anethole is also of interest from a more fundamental standpoint. There are multiple, low-amplitude motions (LAMs) present, including two methyl torsions, a methoxy torsion, and a propenyl torsion. The presence of multiple LAMs becomes an issue when one tries to compute the standard partition function. In a species with small-amplitude motion, one can assume that the vibrational motion is separable. As the range of motion increases, it is less obvious if this assumption holds true. It is a more challenging problem to calculate accurate thermodynamic properties of a system with LAMs than a system that has none. Studies of vibrational modes of anethole will help explore the relations and coupling of multiple, unique LAMs.[4]

The study of LAMs can be facilitated by the use of jet-cooled spectroscopy.[5−8] A jet-cooled molecule will have almost all of its population in the zero-point level, leading to very few hot bands and a simplified vibronic spectrum as compared to the case at room temperature. The jet-cooled vibronic spectroscopy of anethole was initially studied by Grassian et al.; however, their analysis only focused on the excitation spectra.[8] In their work, two possible electronic origin transitions were identified. These origins, separated by 69 cm^{-1}, were attributed to the syn

Received: September 22, 2013
Revised: November 4, 2013
Published: November 4, 2013

   dx.doi.org/10.1021/jp409455e | *J. Phys. Chem. A* 2013, 117, 12831−12841

and anti conformations, with the syn being the lower of the two. This assignment was made by analogy to 3-methylstyrene[8] and *m*-cresol.[9] In both, the conformer with the lowest barrier to methyl torsion was assigned to the less sterically hindered conformer (anti).

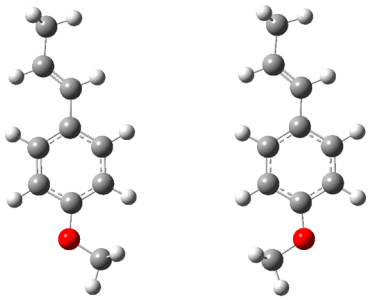

In the current study, we have expanded the analysis of anethole to include laser-induced fluorescence excitation and emission spectroscopy as well as ab initio calculations. The goal of this work is to assign the low frequency modes of anethole in the ground and first excited states, determine geometric parameters for these states, and qualitatively assess the coupling of the observed LAMs.

II. METHODS

The current work employed standard jet-cooling techniques, and therefore a brief description will be given here.[10,11] Anethole (Eastman) was introduced into the fluorescence chamber via Series 9 General Valve (150 μm orifice) operating at 30 Hz. Samples were entrained in helium with a stagnation pressure of 2.5 bar. The vapor pressure of anethole was increase by resistively heating a sample cell to 70 °C. The free-jet expands into a vacuum chamber evacuated by a 6 in. diffusion pump and is crossed by a UV laser at ∼10 nozzle diameters downstream.

Fluorescence spectra were acquired using the doubled output of an N_2-pumped dye laser operating with Rhodamine 610 or Rhodamine 590 laser dyes. Typical laser power in the UV was <25 μJ/pulse. Fluorescence was imaged through a cutoff filter (WG320) and onto a UV sensitive photomultiplier tube (PMT). The PMT response was plotted as a function of laser wavelength to yield a laser-induced fluorescence (LIF) excitation spectrum. Typically, four scans of a region were coadded to yield a final spectrum, with each point of a scan being a 60 laser shot average. The observed laser power did not allow for the acquisition of high quality emission spectra. Therefore, we acquired single vibronic level fluorescence (SVLF) spectra at Purdue University using higher laser fluence (∼1 mJ/pulse). The setup at Purdue has been described in detail previously.[11] This system utilized a larger valve orifice (800 μm) and operated at 20 Hz.

The excitation spectra possess transitions due to all conformational isomers present in the expansion-cooled mixture. UV−UV hole-burning spectroscopy (UVHB) was used to determine the number of isomers present and obtain their individual UV spectral signatures. In UVHB experiments, a tunable dye laser operating at 10 Hz was fixed on a particular $S_1 \leftarrow S_0$ vibronic transition in the excitation spectrum. The power of this hole-burning laser (0.5 mJ/pulse) was sufficient to partially saturate the transition. The probe laser (20 Hz) was tuned across the $S_1 \leftarrow S_0$ vibronic transitions of interest. The probe laser detected depletion of the ground state population when the probe laser was resonant with a transition that shared the same ground state level as the transition on which the hole-burn laser was set. The difference between the signal with and without the hole-burn laser present was monitored using active baseline subtraction with a Boxcar gated integrator. UVHB spectra were recorded using the Purdue fluorescence setup, utilizing Nd^{3+}:YAG pumped dye lasers for the hole-burn and probe beams.

Assignments of SVLF spectra were aided by comparison with density functional theory (DFT) calculations. These calculations employed the B3LYP functional[12,13] with the 6-311++G(d,p) Pople type basis set.[14] Ground state geometries, energies, and harmonic frequencies were calculated using the Gaussian suite of programs.[15] True minima on the potential energy surface were determined by the lack of imaginary frequencies. Excited state calculations were performed using configuration-interaction singles (CIS)[16] and time dependent density functional theory (TD-DFT).[17] Harmonic frequencies were calculated at both levels of theory; however, they were less useful in quantitative predictions of excited state vibrations as compared to ground state methods.

Potential energy surfaces (PES) of the propenyl and methoxy torsional modes were calculated using relaxed potential energy scans. PESs were calculated using B3LYP (as above) and Møller−Plesset, second-order perturbation theory (MP2)[18] using the 6-311+G(d,p) basis set. The torsional angle was stepped by 10°, and the energy is calculated after the remaining coordinates were optimized. The transition state of the PES was compared to the transition state calculation (QST3 keyword) to confirm these surfaces adequately represent the pathways for isomerization between the syn and anti conformers. G4 calculations[19] were performed on the minima and predicted transitions states in an attempt to calculate energetics with high accuracy.

III. RESULTS AND ASSIGNMENTS

Both conformers of anethole are predicted to be heavy-atom planar in the ground state (S_0) by DFT calculations and belong to the C_s point group. The vibrations of anethole ($3N - 6 = 63$) divide into A′ (ν_1–ν_{41}) and A″ symmetry (ν_{42}– ν_{63}), which can generally be described as in- and out-of-plane motions, respectively (Table 1). Assuming the excited state is also of C_s symmetry, electric dipole selections rules dictate that all A′ fundamental vibrations are allowed whereas only even quanta of A″ vibrations or combination bands are allowed. Mulliken notation[20] will be used in assigning vibronic transitions and, when appropriate, Wilson descriptions[21] of benzene like vibrations will also be given in brackets. Assignments of the syn conformer of anethole will precede the anti unless otherwise noted.

A. Excitation Spectrum. The LIF excitation spectrum of the anethole was recorded between 32 800 and 33 800 cm^{-1} (Figure 1a). This region shows two intense transitions at low excitation energies (32 889 and 32 958 cm^{-1}), in agreement with previous results.[8] No transitions were found red of the band at 32 889 cm^{-1}. Several medium to intense bands were observed in this 1000 cm^{-1} spectral region. These transitions tend to appear in pairs, separated by roughly 70 cm^{-1}, indicating there were two molecular conformations in the expansion. UVHB was performed to show the existence of two overlapping spectra with suspected origins at 32 889 and 32 958 cm^{-1} (Figure 1b,c). The transitions were confirmed to be the electronic origins of the syn and anti conformations by SVLF spectroscopy and comparison to computational results

Table 1. Assigned Vibrational Frequencies of Anethole[a]

	syn			anti			
	calc	exp		calc	exp		
	B3LYP	S_0	S_1	B3LYP	S_0	S_1	description[b]
				A″ Symmetry			
63	29	24.0		36	32.0		PP torsion
62	71	71.0	51.0	78	76.0		MeO torsion
61	111	111	124.0	115	112		γ PP
60	186	176	148	186	176	144	PP methyl torsion
59	206			206	201		γ MeO
58	249	246	236	249	248		MeO methyl torsion
56 [16a]	423	409		427	416		ring deform.
				A′ Symmetry			
41	122	122	130	125	124	132	β PP
40	248	242		242	234		βMeO
39	327	325	307	319	317	306	β PP + ring
38	383			410	407	393	β C═C—C + β C—O—C
37	501	504	483	473	473		β C═C—C + β C—O—C
36 [6a]	570	569	540	587	581	536	βPP + MeO + ring
35 [6b]	652	644	594	652	644	585	ring
34	771	770	748	766	763		X-sens stretch
33 [1]	852	851	817	852	849	819	X-sens ring breath
30 [18b]	1061	1055		1061	1055		MeO methyl stretch + ring C—C stretch
25	1233	1218		1235	1232		aryl β CH + C(1)—C(α) stretch

[a]Shown here are the unscaled, calculated frequencies (B3LYP/6-311++G(d,p)), experimentally measured frequencies (S_0 and S_1), and approximate descriptions. All frequencies are in wavenumbers. Assignments are listed using Mulliken notation and Wilson notation, when appropriate. A complete listing of vibrations can be found in the Supporting Information. [b]Notation: PP = propenyl group, MeO = methoxy group, X = both PP and MeO. γ = out-of-plane bend, β = in-plane bend.

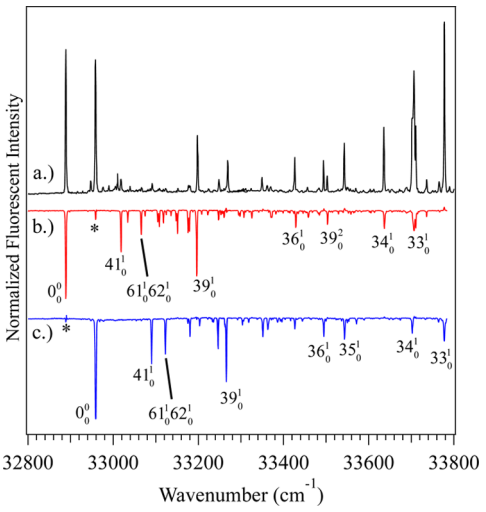

Figure 1. (a) LIF excitation spectrum of anethole (black trace), (b) UVHB spectrum recorded with the hole-burn laser parked on the transition at 32 889 cm^{-1} (red trace), and (c) UVHB spectrum recorded with the hole-burn laser parked on the transition at 32 958 cm^{-1} (blue trace). The spectra have been offset for clarity. The features marked (*) are leak-through from the other isomer that result from incomplete subtraction. Intensity differences between the LIF excitation and UVHB spectra can be attributed to saturation effects (in UVHB) and differences in power curves of the dye lasers.

(section III.B.1). This assignment is also consistent with vertical excitation calculations (TD-DFT, B3LYP/6-311++G(d,p)), which predict the syn origin to be red of the anti origin (calculated 35 061 and 35 573 cm^{-1}, respectively). The most intense bands observed are generally assigned to A′ vibrations, whereas A″ vibrations tend to be much weaker (Table 2). Many more transitions were observed under saturated conditions, as can be seen in this hole-burning spectra (Figure 1b,c).

The intensity of the electronic origins is noticeably different than what was previously observed.[8] Our calculations indicate the two conformers are close in energy (B3LYP = 67 cm^{-1}, MP2 = 2 cm^{-1}, and G4 = 55 cm^{-1}, all zero-point corrected), with the anti being the lower. We therefore expect the pre-expansion conformational populations to be similar, but favoring the anti conformation. This would suggest the anti conformer should show the greatest intensity. In our spectra, the syn conformer has higher intensity, which may indicate a difference in fluorescence quantum yields of the two isomers. As the two studies use different detection schemes (fluorescence vs REMPI), the most likely reason for the observed discrepancies in intensity lies in the differences of fluorescence quantum yields and ionization efficiencies of the two isomers.

The vibronic activity of anethole shows features common to substituted benzenes, particularly; bands can be identified as ring modes, or substituent-sensitive stretches and bends. For example, the 36_0^1 [$6a_0^1$] ring mode was observed at 540 and 536 cm^{-1} whereas the 39_0^1, an in-plane propenyl bend, was observed at 307 and 308 cm^{-1} in the syn and anti conformers, respectively. The [12_0^1] and [$18a_0^1$] benzene-like modes, which are often strong, are notably missing in our assignments. These vibrations are generally found between 920 and 980 cm^{-1}. Transitions were observed in this region, but their intensities precluded unambiguous assignment by SVLF analysis. The low intensity of the [12_0^1] and [$18a_0^1$] benzene-like modes is not

dx.doi.org/10.1021/jp409455e | J. Phys. Chem. A 2013, 117, 12831−12841

Table 2. Frequencies, Normalized Intensities, and Assignments of the LIF Excitation Spectrum of Anethole (All Frequencies in Wavenumbers)

frequency	rel freq[a]	norm intensity	assignment	conformer
32 889	0	100.0	0_0^0	syn
32 928	39	0.7	H_2O[b]	syn
32 947	58	7.6	H_2O[b]	syn
32 958	69	92.9	0_0^0	anti
32 976	87	3.4	H_2O[b]	?
32 990	101	4.3	H_2O[b]	?
33 005	116	3.9	H_2O[b]	?
33 011	122	24.4	H_2O[b]	anti
33 019	130	8.9	41_0^1	syn
33 034	145	1.4	62_0^2	syn
33 039	150	3.9	H_2O[b]	anti
33 066	177	2.8	$61_0^1 62_0^1$	syn
33 091	202	5.9	41_0^1	anti
33 109	220	2.4		syn
33 123	234	2.3	$61_0^1 62_0^1$	anti
33 152	263	2.5		syn
33 176	287	4.1	$58_0^1 62_0^1$	syn
33 180	291	4.3	60_0^2	syn
33 198	309	39.7	39_0^1	syn
33 223	334	2.1		syn
33 247	358	8.7	60_0^2	anti
33 266	377	22.1	39_0^1	anti
33 350	461	10.1	38_0^1	anti
33 361	472	4.2		anti
33 372	483	3.6	37_0^1	syn
33 429	540	24.0	36_0^1	syn
33 456	567	2.9		syn
33 483	594	2.6		syn
33 494	605	22.1	36_0^1	anti
33 504	615	11.1	39_0^2	syn
33 543	654	34.2	35_0^1	anti
33 637	748	45.4	34_0^1	syn
33 702	813	51.8	34_0^1	anti
33 706	817	85.1	33_0^1	syn
33 710	821	46.5		syn
33 739	850	8.5		anti
33 778	889	119.3	33_0^1	anti

[a]Relative frequencies indicate the difference in frequency with respect to the syn origin. [b]Assignment of H_2O indicates the peak is due to a van der Waals cluster of anethole and water.

surprising and has been observed in other para-substituted benzenes.[22,23]

A cooling study was undertaken to ascertain which low frequency bands corresponded to cold, bare-molecule transitions (Figure 2). At low backing pressure (~0.5 bar) bands grow into the spectrum at 0_0^0 + 27, 88, 142, and 150 cm^{-1} (syn) and at 0_0^0 − 20 and 57 cm^{-1} (syn). These features are hot band transitions that arise from population in the v″ = 1 of the ν_{63} or ν_{62}. The SVLF spectra of the largest hot bands were recorded. The analysis of these bands will be presented in section III.B.2. Also observed was the loss of bands at 0_0^0 + 57 and 122 cm^{-1} (syn). The reduced intensity of these bands at lower backing pressure (higher expansion temperature) implies van der Waals clusters. These clusters have identified as anethole/$(H_2O)_n$, but the nature of these clusters is outside the scope of this study and will be presented elsewhere.

B. Single Vibronic Level Fluorescence Spectra. *1. 0^0 SVLF Spectra.* The electronic origin transitions for *syn*- and

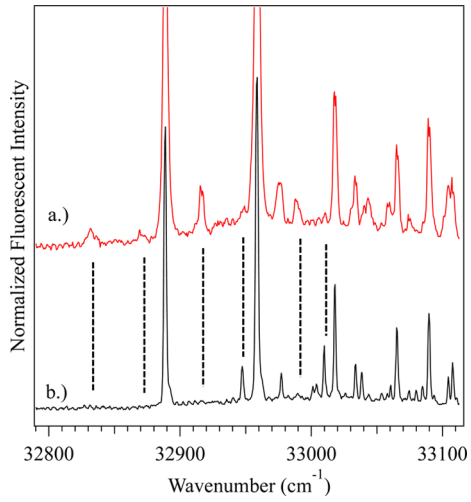

Figure 2. LIF excitation spectrum take under (a) warm and (b) cold expansion conditions. Under warmer conditions, several transitions grow in and several disappear. These differences are highlighted using tie lines. The spectra have been offset for clarity.

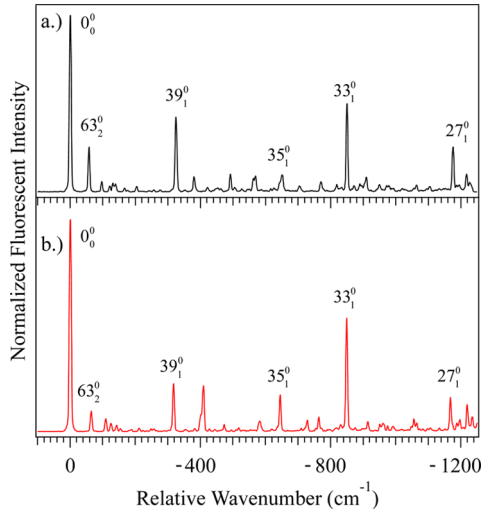

Figure 3. SVLF of the transitions at (a) 32 958 cm^{-1} (red) and (b) 32 889 cm^{-1} (black). The frequency shift shown is relative to the laser excitation frequency. Both spectra are indicative of electronic origins and confirm the existence of two species in the expansion. The similarities of the spectra point toward two rotamers of anethole.

anti-anethole were confirmed by SVLF spectroscopy (Figure 3). The SVLF spectra of these two transitions show marked similarities and subtle differences (Table 3) as expected for a rotamer pair. The emission is characterized by having the most intense feature at the laser resonance, with few intense bands and many weak features. In both spectra, the second most intense band (~50% of the origin transition) is near 850 cm^{-1} (syn at 851, anti at 849) and has been assigned as the 33_1^0 $[1_1^0]$. Other in-plane, benzene-like vibrations were also identified but were of much lower intensity and were less similar in frequency. These assignments were guided by comparison to similar molecules (*trans*-β-methylstyrene,[24,25] anisole,[26] and *p*-coumaryl alcohol[27]) and calculated harmonic frequency (B3LYP/6-311++G(d,p)).

The lowest frequency (0_0^0 − 58 (syn), 0_0^0 − 65(anti)) band observed was assigned to the first overtone of propenyl torsion vibration (63_2^0). This assignment is in good agreement with the calculated vibration frequencies (ν_{63} = 29 cm^{-1} (syn), 36 cm^{-1} (anti)).

dx.doi.org/10.1021/jp409455e | J. Phys. Chem. A 2013, 117, 12831−12841

Table 3. Assignments for the Syn and Anti Origin SVLF Spectra

syn origin: 32 889 cm^{-1}			anti origin: 32 959 cm^{-1}		
rel freq[a]	intensity	assignment	rel freq[a]	intensity	assignment
0	100.0	0_0^0	0	100.0	0_0^0
58	25.6	63_2^0	65	9.7	63_2^0
97	5.9	$62_1^0 63_1^0$	108	6.1	$62_1^0 63_1^0$
122	3.3	41_1^0	124	3.8	41_1^0
131	4.9	63_4^0	141	3.0	62_2^0
139	4.5	62_2^0	153	1.4	
167	2.1	$62_1^0 63_3^0$	188	0.9	$61_1^0 62_1^0$
177	0.7	$61_1^0 62_1^0$	212	1.5	$60_1^0 63_1^0$
205	3.2	$60_1^0 63_1^0$	222	0.4	61_2^0
242	0.6	40_1^0	235	0.4	
256	1.1	$60_1^0 62_1^0$	247	1.3	40_1^0
277	1.1	$59_1^0 62_1^0$	256	1.2	$60_1^0 62_1^0$
325	42.6	39_1^0	317	22.6	39_1^0
353	1.1	60_2^0	355	0.9	60_2^0
380	8.7	$39_1^0 63_2^0$	382	1.6	$39_1^0 63_2^0$
422	2.5	$39_1^0 61_1^0 62_1^0$	402	8.2	59_2^0
455	2.3	$58_1^0 59_1^0$	409	21.7	38_1^0
463	1.7		427	1.3	
492	10.2	58_2^0	472	3.4	$38_1^0 63_2^0$
505	2.5	37_1^0	494	0.8	
526	1.7		516	1.8	
563	7.7		581	4.9	36_1^0
569	9.1	36_1^0	618	1.2	39_2^0
616	1.7		644	17.4	35_1^0
626	2.3		709	1.6	$35_1^0 63_2^0$
642	5.0	35_1^0	728	5.5	$38_1^0 39_1^0$
651	9.8	39_2^0	754	1.6	
704	3.4	$39_2^0 63_2^0$	763	7.0	34_1^0
770	5.7	34_1^0	817	1.8	38_1^0
819	4.3	$39_1^0 58_2^0$	831	3.4	
833	2.6		849	53.6	33_1^0
851	50.1	33_1^0	874	1.9	
871	3.4		896	1.4	
889	4.3		913	4.8	$33_1^0 63_2^0$
910	8.4	$33_1^0 63_2^0$	950	3.4	$33_1^0 61_1^0 62_1^0$
950	4.3	$33_1^0 61_1^0 62_1^0$	959	3.9	
972	3.6	$33_1^0 41_1^0$	975	2.7	$33_1^0 41_1^0$
978	3.6		990	2.5	
993	2.0		1047	2.4	
1021	1.9		1055	5.9	
1028	1.4		1064	4.1	
1056	2.1		1082	1.3	
1063	3.8		1097	1.5	
1096	1.7		1106	1.6	
1105	3.0		1133	1.7	
1176	25.5	$33_1^0 39_1^0$	1167	16.3	$33_1^0 39_1^0$
1186	3.9		1187	4.0	
1195	3.9		1196	5.7	
1218	10.0	25_1^0	1218	12.9	25_1^0

[a]Relative frequency is defined as the red shift from the excitation frequency.

The intensity of the torsional vibration is significantly greater in the syn conformer than the anti. These differences proved useful in assigning SVLF spectra to a specific conformer. A second diagnostic transition was the 39_1, which is found at $0_0^0 - 325$ (syn) and $0_0^0 - 317$ (anti). This vibration is an in-plane bend of the propene moiety with slight ring deformation [6a]. It should be noted that these diagnostic modes are very similar to those observed in *trans*-β-methylstyrene (TBMS). In TBMS, the torsional transition, 42_2^0, was observed at 67 cm^{-1}, whereas the propene bending, 28_1^0, was observed at 347 cm^{-1}. This similarity of frequency indicates that the methoxy and propenyl motions are, to a large degree, uncoupled. A majority of the origin SVLF spectra could be assigned using the computed vibrational frequencies and comparison to similar molecules.

The low frequency region of the SVLF spectrum was assigned by comparison of assignments of similar molecules and calculated harmonic frequencies. The $0_0^0 - 97$ (syn) and $0_0^0 - 108$ (anti) are assigned to the $62_1^0 63_1^0$, as seen in 4-methoxystyrene[28] at 115 and 129 cm^{-1}, respectively. These also fit well with the calculated spacings of 100 and 113 cm^{-1}. The band at $0_0^0 - 122$ (syn) and anti $0_0^0 - 124$ (anti) have been assigned to the lowest in-plane mode, 41_1^0, in good agreement with calculation (122 and 125 cm^{-1}) with the analogous vibration of TBMS (122 cm^{-1}).[24]

2. SVLF Spectra of Hot Bands. Assignment of the out-of-plane modes of the syn conformer was facilitated by the analysis of hot band SVLF spectra (Table 4 and Supporting Information). Emission spectra of $0_0^0 + 27$ and $0_0^0 - 20$ (with respect to the syn origin) were observed to be identical in absolute frequency (Figure 4), indicating the bands share a common upper state but originate from different ground state levels. Moreover, the appearance of progressions of ~325 cm^{-1} indicate spectra both are due to the syn conformer. If we assume the $0_0^0 - 20$ cm^{-1} (syn) is of the type X_1^1, and $0_0^0 + 27$ cm^{-1} (syn) is of the type $X_0^1 Y_1^0$, we can make reasonable determination of the states involved. Here, we find $\tilde{\nu}'_X - \tilde{\nu}''_Y = 27$ cm^{-1} and $\tilde{\nu}'_X - \tilde{\nu}''_X = -20$ cm^{-1}. The difference of these two equations, $\tilde{\nu}''_X - \tilde{\nu}''_Y = 47$ cm^{-1}, gives us the difference in the ground state vibrational frequencies. Even in a warmed expansion, only the lowest states should have population; therefore, it is likely they arise from either the ν_{62} or ν_{63}. Our analysis of the propenyl torsion (seciton IV.B) has given us a value of $\tilde{\nu}''_Y = \tilde{\nu}''_{63} = 24$ cm^{-1}, so we can calculate $\tilde{\nu}''_X = \tilde{\nu}''_{62} = 71$ cm^{-1}. These values are consistent with the calculated (B3LYP) values of 29 and 71 cm^{-1}. Therefore, we assign the $0_0^0 - 20$ cm^{-1} (syn) as 62_1^1, and $0_0^0 + 27$ cm^{-1} (syn) to the $62_0^1 63_1^0$. This assignment is also consistent with the observed intensity of these two bands as we would expect the $62_0^1 63_1^0$ to have more population from the Boltzmann factor. From these assignments, we deduce $\tilde{\nu}'_{62} = 51$ cm^{-1}, which is in suitable agreement with anisole.[26]

A third hot band was observed at $0_0^0 + 100$ cm^{-1} (syn). This band is relatively intense and therefore would seem likely to originate from the 63_1. This assumption yields an excited state vibrational frequency of 124 cm^{-1}, which could correspond to 61^1 or 60^1. We choose to assign this band as the $61_0^1 63_1^0$ based assignments of cold SVLF bands. The SVLF spectra of all three hot bands show several high intensity bands as opposed to a singular false origin. This indicates Duschinsky mixing[29] of these modes, which complicates the analysis of the out-of-plane modes. Unfortunately, all of the hot bands recorded originate from the syn conformer making it difficult to assign the analogous vibrations of the anti conformer. A possible anti hot band may be found $0_0^0 + 17$ cm^{-1} (anti). It would be reasonable to assume that this is the $62_0^1 63_1^0$. Additional hot bands of the anti conformer could not be determined due to spectral congestion of the LIF excitation spectrum.

3. SVLF Spectra of Cold Bands. As the vibronic activities of the conformers are similar, we will present arguments and assignments for the syn conformer and note difference in anti

Table 4. Representative Assignments (41^1_0, $61^1_0 62^1_0$, and $62^1_0 63^0_1$) of the SVLF Spectra of *syn*-Anethole[a]

0^0_0 + 130 cm^{-1} (33 019 cm^{-1})		0^0_0 + 177 cm^{-1} (33 066 cm^{-1})		0^0_0 + 27 cm^{-1} (32 916 cm^{-1})	
rel freq[b]	assignment	rel freq[b]	assignment	rel freq[b]	assignment
0	41^1_0	0	$61^1_0 62^1_0$	0	$62^1_0 63^0_1$
58	$41^1_0 63^0_2$	59	$61^1_0 62^1_0 63^0_2$	89	62^1_1
102		96		157	$62^1_1 63^0_3$
107		130	$61^1_0 62^1_0 63^0_4$	178	
121	41^1_1	165		220	6112 6301
139	$41^1_0 62^0_2$	181	$61^1_1 62^1_1$	324	$39^0_1 62^1_0 63^0_1$
150		208	$61^1_0 62^1_0 63^0_6$	412	$39^0_1 62^1_1$
176	$41^1_1 63^0_2$	222	$61^1_2 62^1_0$	443	$39^0_1 61^1_1 63^0_3$
244	41^1_2	249	?	484	
251	$41^1_1 63^0_4$	274		652	$39^0_2 62^1_0 63^0_1$
259	$41^1_1 62^0_2$	280	$61^1_1 62^1_2 63^0_1$	719	
287	$41^1_1 62^0_1 63^0_3$	291		729	$35^0_1 62^1_1$
297	41^1_1	321		741	
324	$39^0_1 41^1_0$	364	$61^1_2 62^1_2$	810	
379	$39^1_0 41^1_0 63^0_2$	417		826	
395		452		849	$33^0_1 62^1_0 63^0_1$
428		462		882	
447	$39^0_1 41^1_1$	489	$58^0_2 61^1_1 62^1_1$	937	$33^0_1 62^1_1$
499	$39^0_1 41^1_1 63^0_2$	508	$39^0_1 61^1_1 62^1_1$	1007	$33^0_1 62^1_1 63^0_3$
532		531	$39^0_1 61^1_0 62^1_0 63^0_6$	1031	
540		549	$39^0_1 61^1_2 62^1_0$	1059	
568	$36^0_1 41^1_0$	575	$249 + 39^0_1$	1069	
573		774		1175	
584		848			
614	$41^1_1 58^0_2$	908			
647		948			
686		979			
692	$36^0_1 41^1_1$	985			
708		1013			
746		1031	$33^0_1 61^1_1 62^1_1$		
753		1059	$33^0_1 61^1_1 62^1_1 63^0_6$		
766		1073	$33^0_1 61^1_2 62^1_0$		
773	$39^1_2 41^1_1$	1099	$249 + 33^0_1$		
821		1128			
826		1147			
849	$33^0_1 41^1_0$	1173			
893					
939					
945					
972	$33^0_1 41^1_1$				
992					
1018					
1026	$33^0_1 41^1_1 63^0_2$				

[a]Full assignments are given in the Supporting Information. [b]Relative frequency is defined as the red shift from the excitation frequency.

when appropriate. Complete tables of experimental frequencies (syn and anti) along with all anti SVLF spectra can be found in the Supporting Information. In-plane modes were quickly identified by observation of relatively simple vibronic activity. This is in stark contrast to the SVLF spectrum of out-of-plane vibrations. The 0^0_0 + 130, 0^0_0 + 309, and 0^0_0 + 540 cm^{-1} (syn) bands observed in the excitation spectrum of the syn conformation were assigned to the in-plane fundamentals 41^1_0, 39^1_0, and 36^1_0, respectively (Figure 5a). The SVLF spectrum of the 41^1_0 shows a false origin at 41^1_0 − 121 cm^{-1} (syn) with additional structure that mirrors the SVLF spectrum of the origin band

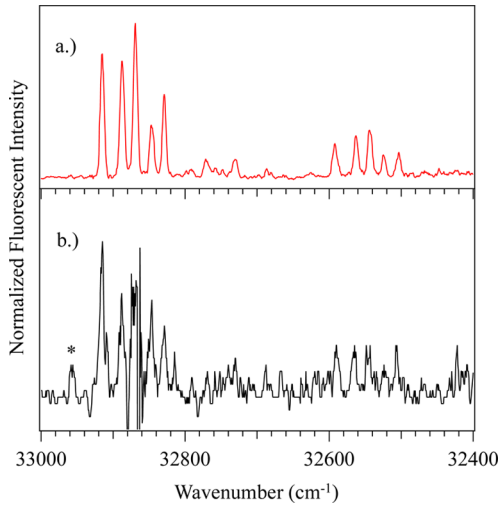

Figure 4. SVLF spectra of the hot band transitions at (a) 0^0_0 + 27 (syn) and (b) 0^0_0 − 20 cm^{-1} (syn). The transitions of both spectra have identical absolute frequencies, indicating they share a common excited state and have been assigned to $62^1_0 63^0_1$ and 62^1_1, respectively. The feature marked (*) is an artifact that appears in every SVLF spectra and is apparent here due to low signal-to-noise.

SVLF spectrum. The 36^1_0 shows similar behavior, with a false origin at 36^1_0 − 568 cm^{-1} (syn). The 308 and 615 cm^{-1} spectra were observed to have strong progressions of 325 cm^{-1}, indicating the 308 cm^{-1} to be the fundamental and 615 cm^{-1} to be an overtone. These transition were assigned as the 39^1_0 and 39^2_0, respectively. Similar logic was used to assign the SVLF spectra of 0^0_0 + 132, 0^0_0 + 308, and 0^0_0 + 585 cm^{-1} (anti) transitions of the anti conformer to 41^1_0, 39^1_0, and the 35^1_0, respectively.

The SVLF spectrum of the 36^1_0 (syn) shows sharp structure superimposed upon broad structure. This broad background is most likely due to intermolecular vibrational redistribution (IVR). Emission spectra of bands above this level tend to show increased broad structure and fewer sharp features. The 0^0_0 + 748 cm^{-1} (syn) is dominated by the broad structure but still shows a possible false origin with a red shift of 770 cm^{-1} and was thus assigned as the 34^1_0. Similar broad structure is observed in the anti conformer. The appearance of broad features with increasing frequency is useful in assigning the 0^0_0 + 481 cm^{-1} (syn) transition. This band could be reasonably assigned to the 58^2_0 or the 37^1_0, but the appearance of broad features favors the assignment as a fundamental.

The out-of-plane vibrations tend to be more difficult to unambiguously assign due to Duschinsky mixing (Figure 5b). The SVLF of A″ modes tend to show complex structure, lack a clear false origin, and are much weaker than A′ bands. This general behavior is observed in the 0^0_0 + 177, 0^0_0 + 219, 0^0_0 + 263, 0^0_0 + 288, and 0^0_0 +291 cm^{-1} (syn) as well as 0^0_0 + 164 and 0^0_0 + 290 cm^{-1} (anti). What is presented here best fits the available data for the out-of-plane modes but should not be considered firm assignments. Our assignments start from the syn hot band spectra, which gave us fundamental frequencies for ν'_{62} and ν'_{61}. These frequencies allow us to assign the 0^0_0 + 177 cm^{-1} (syn) to $61^1_0 62^1_0$. The SVLF spectrum of the 0^0_0 +177 cm^{-1} (syn) band shows the strongest emission feature red-shifted by 181 cm^{-1}, which is reasonable to assign as the $61^1_1 62^1_1$. The 0^0_0 + 164 cm^{-1} (anti) was assigned as the $61^1_0 62^1_0$, by analogy to the 0^0_0 + 177 cm^{-1} (syn). However, the strongest band in the 0^0_0 + 164 cm^{-1}

dx.doi.org/10.1021/jp409455e | J. Phys. Chem. A 2013, 117, 12831−12841

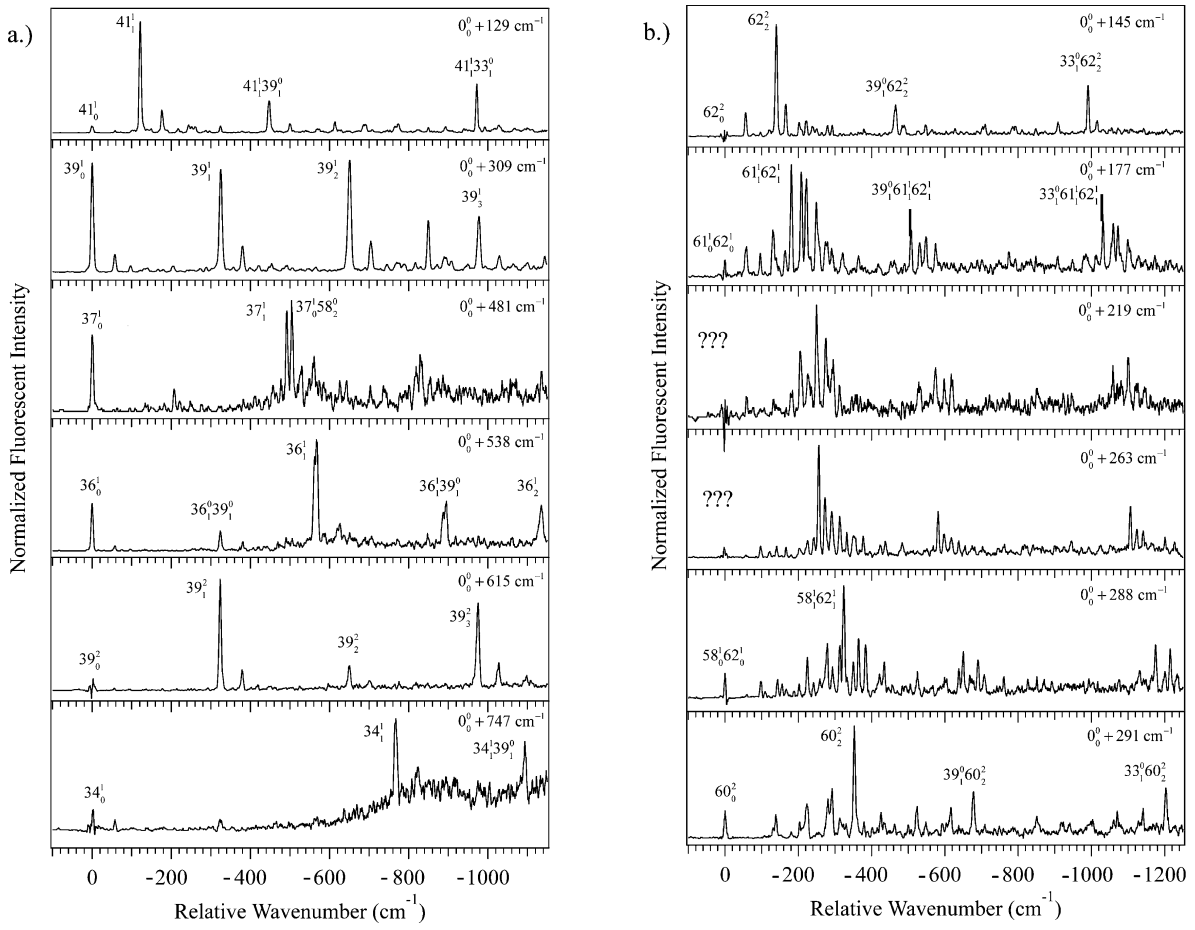

Figure 5. SVLF spectra of (a) in-plane and (b) out-of-plane modes of *syn*-anethole. The frequency shift shown is relative to the laser excitation frequency. The in-plane modes are noted to have generally simpler spectra with firm assignments. The out-of-plane modes show a large degree of mixing, making assignments less certain. Two unassigned bands are shown here to stimulate discussion. Full assignments can be found in the Supporting Information.

(anti) spectrum is not $61^1_1 62^1_1$, but rather $60^0_1 61^1_0 62^1_0 63^0_1$. This assignment is plausible by assuming that Duschinsky mixing is present in the anti conformer as well as the syn conformer. The 0^0_0 + 291 (syn) and 0^0_0+ 290 (anti) cm^{-1} are assigned as the 60^2_0. These transitions show strong emission red-shifted by 352 cm^{-1}, which could reasonably be assigned to the 60^2_2 by comparison to calculations and the SVLF spectra of TBMS. This mode is best described as a torsional motion of the propenyl methyl group and is analogous to the ν_{49} of TBMS.[25]

The 0^0_0 + 288 cm^{-1} (syn) shows its strongest emission feature red-shifted by 324 cm^{-1}. This spectrum also shows a great deal of vibronic activity and cannot be assigned using A′ modes, therefore implying it originates from an overtone or combination band of A″ modes. It seems strange that the emission should go to an A′ mode and could indicate an atypical coupling of modes. An alternative explanation is to assign this as $58^1_0 62^1_0$. This assignment is plausible given our ab initio calculations, which are consistent with this combination band occurring at 324 cm^{-1}. The SVLF spectrum of 0^0_0 + 145 cm^{-1} (syn) is quite different than the rest of the out-of-plane transitions. This band looks more like a false origin spectra and has no easily assigned anti counterpart. We have chosen to assign this transition tentatively as the overtone of the methoxy torsion (62^2_0). This assignment indicates significant anharmonicity as the ν_{62} fundamental was determined to be 51 cm^{-1}. Excited state calculations (CIS and TD-DFT) indicate there is substantial difference in the harmonicity of the methoxy torsion of the two conformers. This difference could lead to the anti conformer being strongly frequency shifted from the syn, hence why it was not observed.

Two bands could not be identified (0^0_0 + 220 and +263 cm^{-1} (syn)) in our analysis. The 0^0_0 + 220 cm^{-1} (syn) emits strongly at −249 cm^{-1} (syn). This level is most likely the $60_1 62_1$, but this does not fit the excited states frequencies for these levels. An accurate assignment of this transition is challenging. It is possible that either of these bands is connected to the 63^1, but without further data, it is less than obvious what modes may be involved. In the absence of further data, we cannot clearly assign these transitions. It would be interesting to acquire more hot band spectra or low frequency IR data to help assign these bands. We present these spectra with unclear assignments to spur further discussion. Transitions observed in these spectra can be found tabulated in the Supporting Information.

IV. DISCUSSION AND ANALYSIS

A. Substituent Effects on the Spectra. The excitation and emission spectroscopy show progressions in ν_{39}, an in-plane bending mode of the propene moiety. The SVLF spectrum of 0^0_0 + 309 cm^{-1} (syn) shows progression of 325 cm^{-1}, with four members, starting with the resonance transition. The bend overtone, found at 0^0_0 + 615 cm^{-1} (syn), also shows a harmonic progression of 325 cm^{-1}. An analysis of the Franck−Condon

dx.doi.org/10.1021/jp409455e | J. Phys. Chem. A 2013, 117, 12831−12841

factors of the ν_{39} can be performed using the method of Henderson[30] to show the degree of displacement along this coordinate upon excitation. This analysis yields a displacement value, D, of 0.95, indicating a substantial displacement in the syn conformer. Interestingly, the Franck−Condon activity in the anti is quite different (Figure 6). Only one quantum of

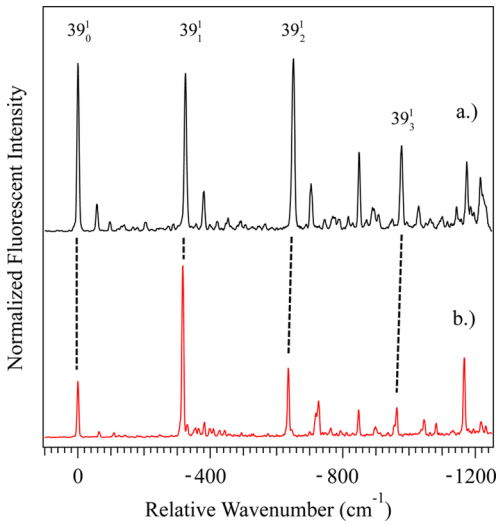

Figure 6. Comparison of the SVLF spectra from 39^1_0 of (a) *syn*- and (b) *anti*-anethole. The frequency shift shown is relative to the laser excitation frequency. Tie lines have been added to indicate the vibrational progression these spectra.

excitation was unambiguously assigned in the LIF excitation spectrum at 0^0_0 + 308 cm^{-1} (anti). The calculated displacement (D = 0.55) for this mode is much lower than the syn conformer, indicating a smaller geometry change upon electronic excitation.

This altered behavior can be rationalized by observation of the calculated molecular orbitals (Figure 7). CIS and TD-DFT calculations indicate that the electronic transition is mostly HOMO → LUMO in character. The general features of the

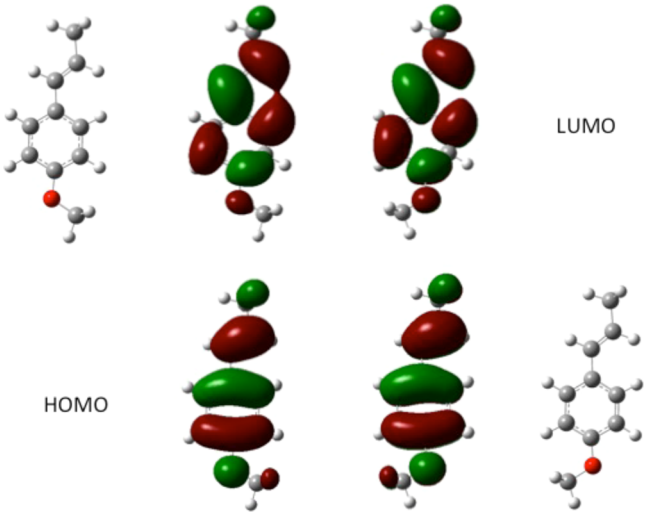

Figure 7. Calculated (B3LYP/6-311++G(d,p)) molecular orbitals involved in the electronic transition of *syn*- and *anti*-anethole. The relative orientation of the methoxy group causes a slight rotation of the molecular orbitals that can be used to explain much of the observed Franck−Condon activity.

HOMO and LUMO are quite similar in both conformers, but closer inspection shows a slight rotation of the orbital contribution of the phenyl ring. The slight rotation leads to more electron density between the ring and the propenyl group in the syn conformer as compared to the anti. The change in density manifests as a larger geometry change upon electronic excitation for one conformer. In essence, the rotation of the methoxy group is influencing a vibrational mode even without being an actual part of the vibration.

There is little evidence for direct coupling of LAMs between the two substituent groups. As can be seen in the mode description (Table 1), there are very few modes that can be described as concerted motion of both substituents. For example, the calculated torsion of the propenyl group (ν_{63}) shows no motion of the methoxy group, whereas the methoxy torsion (ν_{62}) shows only minor motion of the propenyl group. This separation of substituent vibrations is apparent in many spectroscopic assignments for anethole, which are often close in frequency to the assigned vibration of TBMS and anisole (Table 5). This decoupling of substituents is not uncommon in

Table 5. Comparison of Ground State Vibration Frequencies (cm^{-1}) of Anethole and Related Species

	symmetry	syn	anti	TBMS	anisole
propenyl torsion	A″	24	32	28	
MeO torsion	A″	71	76		98
propenyl bend	A′	122	124	144	
MeO bend	A′	242	234		251
propenyl bend	A″	111	112	121	
MeO bend	A″		201		204
propenyl methyl torsion	A″	176	176	189	
MeO methyl torsion	A″	248	246		258

para-substituted systems.[22,23] It would be interesting to compare anethole to a meta or ortho analogue. This study is outside the scope of the current work and may be attempted in the future.

B. Torsional Barriers. Experimental torsional potentials of the S_0 state were simulated by fitting the eigenvalues of an internal rotation Hamiltonian (eq 1) to experimentally observed torsional transition frequencies to obtain the form of the torsional potential in the S_0 state.

$$H\Psi_v = \left[-B\frac{\partial^2}{\partial\phi^2} + V[\phi]\right]\Psi_v = E_v\Psi_v \quad (1)$$

This methodology has been successfully performed for many species where torsional structure was evident.[5−7,31] An unweighted linear-least-squares sum was minimized to fit the simulated spacings to experimental values. The torsional potential is the commonly used truncated Fourier expansion

$$V(\theta) = \frac{1}{2}\sum_n V_n[1 - \cos(n\theta)] \quad (2)$$

Because anethole has been shown to be planar in the ground state by analysis of the out-of-plane vibrations (section III.C), the potential has a minimum at 0° (defined here as the anti conformer) and is symmetric about the minimum. The internal rotation constant, B, was determined by

$$B = \frac{h}{8\pi^2 c I_r^a} \quad (3)$$

dx.doi.org/10.1021/jp409455e | J. Phys. Chem. A 2013, 117, 12831−12841

where I_r is the reduced moment of inertia defined by Pitzer.[32] The propenyl group for the syn and anti conformers differ significantly in internal rotation constant such that the B was derived as a cosine expansion as such

$$B = B_0 + B_1 \cos\theta + B_2 \cos 2\theta \quad (4)$$

Geometric parameters for the syn, anti, and the connecting transition states were taken from B3LYP optimizations and were used to determine values of B_0 = 1.0155, B_1 = −0.0676, and B_2 = 0.0767 cm^{-1}.

Because there are two distinguishable conformers, V_1, V_2, and V_4 were needed to make satisfactory fits of the observed structure. For this system, V_1 indicates the difference in energy of the two conformations, whereas V_2 describes the overall barrier height, and V_4 describes the anharmonicity of the potential (Table 6 and Figure 8). The barrier height (V_2 = 623 cm^{-1}) and anharmonicity (V_4 = −133 cm^{-1}) are substantially lower in magnitude than TBMS[24] and 4-methoxystyrene.[30] If we compare the torsional barriers of styrene[33] and TBMS, a drop in the torsional barrier of 215 cm^{-1} is observed. We expect the torsional barrier of anethole would experience a similar change when compared to 4-methoxystyrene. In the study of 4-methoxystyrene, too few transitions were identified to independently fit the V_2 component, which was instead fixed at a reasonable value of 950 cm^{-1}. We therefore expect the V_2 in anethole to be near 735 cm^{-1}, in agreement with our simulation. The simulated energy difference in the conformer wells (V_1 = 37 cm^{-1}) predicts anti as the lower energy conformer and is in reasonable agreement with B3LYP (67 cm^{-1}) and G4 calculations (55 cm^{-1}). In 4-methoxystyrene, the authors only observed two transitions that could be used in their fits. The use of only two transitions led to two possible solutions for the torsional potential. These solutions differed by which isomer was lower in energy. Because we were able to identify more transitions, we can say with great certainty that the best-fit torsional potential has the anti conformer lower in energy. Simulations were attempted in which the syn isomer was constrained to be the lower energy isomer, but these simulations led to poor fits overall.

Table 6. Comparison of Observed and Calculated Torsional Transitions for Anethole and Fitted Potential Parameters (All Values in Wavenumbers)

syn		anti	
obs	calc	obs	calc
24[a]	24	32[b]	28
58	58	65	65
131	131	135	135
208	208		
V_1	37		
V_2	626		
V_4	−133		

[a]Value determined from analysis of hot band SVLF spectra. [b]Value determined from harmonic description of 63_2.

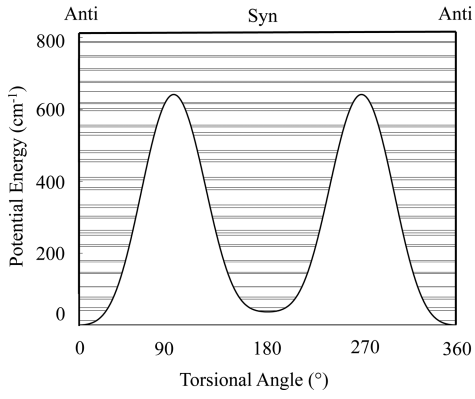

Figure 8. Simulated potential energy surface for the propenyl torsion in the S_0 state.

The calculated frequencies of our simulation are in good agreement with experimental values (Table 6). All fit frequencies deviate by less than 1 cm^{-1} from observed transitions. The derived torsional fundamentals (ν_{63} = 24 cm^{-1} (syn) and ν_{63} = 32 cm^{-1} (anti)) were not explicitly fit in our simulation but were reproduced quite well. The simulated fundamentals were found to be 24 and 28 cm^{-1} for syn and anti, respectively. The anti fundamental shows a larger deviation than all other frequencies, but this is not surprising as the experimental value (Table 1) is based on a harmonic approximation. The syn fundamental was determined from analysis of hot band spectra involving the torsional fundamental and therefore shows better agreement.

The torsional potential energy surface was calculated at several levels of theory with varying results. DFT predicted V_2 = 1360 cm^{-1}, with a single, flat-bottomed well for each conformer. MP2, however, predicts a lower barrier (V_2 = 872 cm^{-1}) and double well minimum for each conformer. In previous studies, styrene-like systems have often shown to have geometry parameters similar to DFT calculations, but energetic barriers that are more accurately represented from MP2.[34,35] In an attempt to determine a more accurate barrier height, G4 energy calculations were performed on each conformer and the transition state connecting the two wells. The G4, zero-point corrected energy difference was determined to be 1047 cm^{-1}. G4 calculations are known to yield highly accurate energies, so it is surprising that this method predicts a barrier farther from the experimental value than MP2 calculations. A more in-depth study of the accuracy of propenyl torsional barriers at the G4 level of theory would be interesting but is beyond the scope of this report.

We were not able to identify torsional transitions in the excited state of anethole. A reasonable explanation would be that the frequency of 63^1 is highly shifted from the ground state value and appear as low intensity features in the excitation spectrum. Because the ground torsional frequency is nearly identical to TBMS[24] it is reasonable to assume the excited state may be similarly unaffected. Thus we could conjecture the 63^2 is found near 330 cm^{-1} above the respective origin. Indeed, under saturated conditions, several transitions can be found in this spectrum, but they were too weak to disperse.

The torsional barrier in the excited state was estimated computationally. Relaxed optimizations of the excited state, however, were less successful than of the ground state. Calculations at the CIS level of theory would not converge when diffuse functions were used; therefore, we present results using the 6-311(d,p) basis set. TD-DFT optimization near the transition state predicted a structure with significant deformation of the propenyl moiety away from the expected transition state.[36] We therefore chose to use the B3LYP potential energy surface and make TD-DFT energy corrections at each geometry. Both CIS and TD-DFT show a near order of magnitude increase in the torsional barrier ($V_{2,CIS}$ = 6874 cm^{-1},

$V_{2,\text{TD-DFT}}$ = 5060 cm^{-1}) inline with expectations. These potentials would predict the 63_0^2 to be found at energies in excess of 0_0^0 + 200 cm^{-1}.

There were too few observable methoxy torsional transitions to simulate torsional potentials. Unlike the propenyl PES, TD-DFT was able to calculate the methoxy PES for the S_1 state. The computed methoxy torsional potentials show an interesting feature. The calculated ground state potential (B3LYP) is adequately fit using the three parameters; however, the excited state (TD-B3LYP) could only be fit using four terms (Table 7). This difference reflects the differences in the harmonicity of each conformer well. In the ground state, the methoxy torsions of the syn and anti conformers have roughly the same degree of anharmonicity. In the excited state, the methoxy vibration is much more anharmonic in the anti well than the syn well. It would be very interesting to obtain more SVLF spectra to see if this difference could be experimentally verified.

Table 7. Calculated Torsion Parameters for the Methoxy Torsion in the Ground and Excited Electronic State (Values in Wavenumbers)

S_0 (B3LYP)		S_1 (TD-B3LYP)	
V_1	74	V_1	334
V_2	1035	V_2	2086
		V_3	244
V_4	148	V_4	−215

To better show the relationship of the methoxy and propenyl torsional systems, we computed (B3LYP) the 2D potential energy surface (Figure 9). Here, we see a lower barrier to isomerization through the methoxy coordinate (V_2 = 1035 vs V_2 = 1360 cm^{-1}). This is most likely due to the enhanced rigidity that is gained through the conjugation of the phenyl ring to the propenyl group. Also apparent is the independence of the two rotor systems. The 2D PES is in agreement with the spectroscopy in that these LAMs are almost entirely orthogonal. A corresponding surface for the excited state was attempted but abandoned due to the aforementioned difficulties in computing PESs involving the propenyl group using CIS and TD-DFT methods.

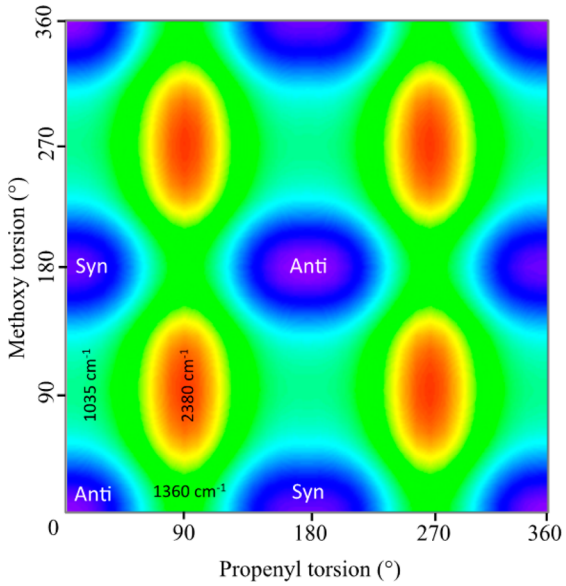

Figure 9. Calculated potential energy surface [B3LYP/6-311++G(d,p)] of the methoxy and propenyl torsional coordinates. The coordinates are almost completely uncoupled, in agreement with the spectral analysis.

V. CONCLUSIONS

The fluorescence excitation and emission spectra of the syn and anti conformations of anethole have been recorded. This work compares fluorescence spectra with ab initio results, along with torsional simulations to confirm the conformational assignments of the syn electronic origin at 32 889 cm^{-1} and the anti origin at 32 958 cm^{-1}, as proposed by Grassian and co-workers.[8] SVLF spectroscopy was used to assign many vibronic bands observed in the LIF excitation spectrum including torsional vibrations of the propenyl and methoxy substituents. Vibronic assignments indicate that both conformers have C_s symmetry in the ground and first excited states. Our analysis shows that although the LAMs are largely decoupled vibrationally, the individual modes can be perturbed by the relative orientation of the substituents. Also observed in this work were several anethole/water clusters, despite the low solubility of anethole in water.

■ ASSOCIATED CONTENT

Supporting Information

Complete listing of vibrational modes of anethole and complete assignments of acquired SVLF spectra. This information is available free of charge via the Internet at http://pubs.acs.org

■ AUTHOR INFORMATION

Corresponding Author

*J. J. Newby: e-mail, jnewby1@swarthmore.edu.

Notes

The authors declare no competing financial interest.

■ ACKNOWLEDGMENTS

The authors gratefully acknowledge support of the Swarthmore College Faculty Research Fund. The authors are grateful to Thomas A. Stephenson and Timothy S. Zwier for the use of laboratory space and equipment. J.J.N. acknowledges Paul R. Rablen for useful discussions of computational methods. V.P.B. acknowledges Swarthmore College for an undergraduate research fellowship that allowed her to complete much of this work. Computational resources of the Extreme Science and Engineering Discovery Environment (XSEDE), a program supported by National Science Foundation grant number OCI-1053575, were used in this work.

■ REFERENCES

(1) Bernards, M. A. Plant Natural Products: A Primer. *Can. J. Zool.* **2010**, *88*, 601−614.

(2) Kubo, I.; Fujita, K.; Nihei, K. Antimicrobial Activity of Anethole and Related Compounds from Aniseed. *J. Sci. Food. Agr.* **2008**, *88*, 242−247.

(3) Ozcan, M. M.; Chalchat, J. C. Chemical Composition and Antifungal Effect of Anise (*Pimpinella Anisum L.*) Fruit Oil at Ripening Stage. *Ann. Microbiol.* **2006**, *56*, 353−358.

(4) Wong, B. M.; Green, W. H. Effects of Large-Amplitude Torsions on Partition Functions: Beyond the Conventional Separability Assumption. *Mol. Phys.* **2005**, *103*, 1027−1034.

(5) Newby, J. J.; Liu, C.-P.; Müller, C. W.; Zwier, T. S. Jet-Cooled Vibronic Spectroscopy of Potential Intermediates Along the Pathway to PAH: Phenylcyclopentadi-1,3-Ene. *Phys. Chem. Chem. Phys.* **2009**, *11*, 8316−8329.
(6) Newby, J. J.; Liu, C. P.; Muller, C. W.; James, W. H.; Buchanan, E. G.; Lee, H. D.; Zwier, T. S. Spectroscopy and Photophysics of Structural Isomers of Naphthalene: Z-Phenylvinylacetylene. *J. Phys. Chem. A* **2010**, *114*, 3190−3198.
(7) Newby, J. J.; Müller, C. W.; Liu, C.-P.; Zwier, T. S. Jet-Cooled Vibronic Spectroscopy and Asymmetric Torsional Potentials of Phenylcyclopentene. *Phys. Chem. Chem. Phys.* **2009**, *11*, 8330−8341.
(8) Grassian, V. H.; Bernstein, E. R.; Secor, H. V.; Seeman, J. I. Conformational Study of Jet-Cooled Styrene Derivatives - Demonstration of the Planarity of Nonsterically Hindered Styrenes. *J. Phys. Chem.* **1989**, *93*, 3470−3474.
(9) Mizuno, H.; Okuyama, K.; Ebata, T.; Ito, M. Rotational Isomers of *m*-Cresol and Internal-Rotation of the CH_3 Group in S_0, S_1, and the Ion. *J. Phys. Chem.* **1987**, *91*, 5589−5593.
(10) Stephenson, T. A.; Simpson, W. R.; Wright, J. R.; Schneider, H. P.; Miller, J. W.; Schultz, K. E. Laser-Induced Fluorescence of Jet-Cooled IBr: $B^3\Pi_{0^+} \leftarrow X^1\Sigma^+$ Excitation-Spectra. *J. Phys. Chem.* **1989**, *93*, 2310−2313.
(11) Pillsbury, N. R.; Muller, C. W.; Meerts, W. L.; Plusquellic, D. F.; Zwier, T. S. Conformational Effects on Excitonic Interactions in a Prototypical H-Bonded Bichromophore: Bis(2-Hydroxyphenyl)-Methane. *J. Phys. Chem. A* **2009**, *113*, 5000−5012.
(12) Becke, A. D. Density-Functional Thermochemistry III. The Role of Exact Exchange. *J. Chem. Phys.* **1993**, *98*, 5648−5652.
(13) Lee, C. T.; Yang, W. T.; Parr, R. G. Development of the Colle-Salvetti Correlation-Energy Formula into a Functional of the Electron-Density. *Phys. Rev. B* **1988**, *37*, 785−789.
(14) Frisch, M. J.; Pople, J. A.; Binkley, J. S. Self-Consistent Molecular-Orbital Methods 0.25. Supplementary Functions for Gaussian-Basis Sets. *J. Chem. Phys.* **1984**, *80*, 3265−3269.
(15) Frisch, M. J.; Trucks, G. W.; Schlegel, H. B.; Scuseria, G. E.; Robb, M. A.; Cheeseman, J. R.; Scalmani, G.; Barone, V.; Mennucci, B.; Petersson, G. A.; et al. *Gaussian 09*, Revision C.01; Gaussian Inc.: Wallingford, CT, 2009.
(16) Foresman, J. B.; Headgordon, M.; Pople, J. A.; Frisch, M. J. Toward a Systematic Molecular-Orbital Theory for Excited-States. *J. Phys. Chem.* **1992**, *96*, 135−149.
(17) Bauernschmitt, R.; Ahlrichs, R. Treatment of Electronic Excitations within the Adiabatic Approximation of Time Dependent Density Functional Theory. *Chem. Phys. Lett.* **1996**, *256*, 454−464.
(18) Moller, C.; Plesset, M. S. Note on an Approximation Treatment for Many-Electron Systems. *Phys. Rev.* **1934**, *46*, 0618−0622.
(19) Curtiss, L. A.; Redfern, P. C.; Raghavachari, K. Gaussian-4 Theory. *J. Chem. Phys.* **2007**, *126*, 0841081−08410812.
(20) Mulliken, R. S. Report on Notation for the Spectra of Polyatomic Molecules. *J. Chem. Phys.* **1955**, *23*, 1997−2011.
(21) Wilson, E. B. The Normal Modes and Frequencies of Vibration of the Regular Plane Hexagon Model of the Benzene Molecule. *Phys. Rev.* **1934**, *45*, 0706−0714.
(22) Selby, T. M.; Meerts, W. L.; Zwier, T. S. Isomer-Specific Ultraviolet Spectroscopy of *m*- and *p*-Divinylbenzene. *J. Phys. Chem. A* **2007**, *111*, 3697−3709.
(23) Patwari, G. N.; Doraiswamy, S.; Wategaonkar, S. IVR in the S_1 State of Jet-cooled *cis*- and *trans*-*p*-Dimethoxybenzene. *Chem. Phys. Lett.* **2000**, *316*, 433−441.
(24) Sinclair, W. E.; Yu, H.; Phillips, D.; Gordon, R. D.; Hollas, J. M.; Klee, S.; Mellau, G. C(1)-C(α) Torsion Potential Function and Vibrational Assignments of *trans*-β-Methylstyrene from S_1-S_0 Supersonic Jet Fluorescence Spectra. *J. Phys. Chem.* **1995**, *99*, 4386−4396.
(25) Haas, Y.; Kendler, S.; Zingher, E.; Zuckermann, H.; Zilberg, S. $S_0 \leftrightarrow S_1$ Transition of *trans*-β-Methyl Styrene: Vibronic Structure and Dynamics. *J. Chem. Phys.* **1995**, *103*, 37−47.
(26) Matsumoto, R.; Sakeda, K.; Matsushita, Y.; Suzuki, T.; Ichimura, T. Spectroscopy and Relaxation Dynamics of Photoexcited Anisole and Anisole-d_3 Molecules in a Supersonic Jet. *J. Mol. Struct.* **2005**, *735*, 153−167.
(27) Rodrigo, C. P.; James, W. H.; Zwier, T. S. Single-Conformation Ultraviolet and Infrared Spectra of Jet-Cooled Monolignols: *p*-Coumaryl Alcohol, Coniferyl Alcohol, and Sinapyl Alcohol. *J. Am. Chem. Soc.* **2011**, *133*, 2632−2641.
(28) Ribeiroclaro, P. J. A.; Teixeiradias, J. J. C.; Hollas, J. M.; Milewski, M. Discovery of 2 Rotational Isomers of 4-Methoxystyrene by Laser-Induced Fluorescence in a Supersonic Jet. *J. Chem. Soc., Faraday Trans.* **1995**, *91*, 197−203.
(29) Duschinsky, F. The Importance of the Electron Spectrum in Multi Atomic Molecules. Concerning the Franck-Condon Principle. *Acta Physicochimica URSS* **1937**, *7*, 551−566.
(30) Henderson, J. R.; Muramoto, M.; Willett, R. A. Harmonic Franck-Condon Overlap Integrals Including Displacement of Normal Coordinates. *J. Chem. Phys.* **1964**, *41*, 580−581.
(31) Lewis, J. D.; Malloy, T. B.; Chao, T. H.; Laane, J. Periodic Potential Functions for Pseudorotation and Internal-Rotation. *J. Mol. Struct.* **1972**, *12*, 427−449.
(32) Pitzer, K. S. Energy Levels and Thermodynamic Functions for Molecules with Internal Rotation: II. Unsymmetrical Tops Attached to a Rigid Frame. *J. Chem. Phys.* **1946**, *14*, 239−243.
(33) Hollas, J. M. Progress in Electronic Spectroscopy of Large Molecules. *J. Chem. Soc., Faraday Trans.* **1998**, *94*, 1527−1540.
(34) Müller, C.; Klöppel-Riech, M.; Schröder, F.; Schröeder, J.; Troe, J. Fluorescence and Rempi Spectroscopy of Jet-Cooled Isolated 2-Phenylindene in the S_1 State. *J. Phys. Chem. A* **2006**, *110*, 5017−5031.
(35) Liu, C.-P.; Newby, J. J.; Müller, C. W.; Lee, H. D.; Zwier, T. S. Spectroscopic Characterization of Structural Isomers of Naphthalene: (*E*)- and (*Z*)-Phenylvinylacetylene. *J. Phys. Chem. A* **2008**, *112*, 9454−9466.
(36) It is of interest that CIS and TDDFT have trouble producing potential energy surfaces for anethole. This could indicate close lying electronic states that play a role in the isomerization between the two conformations.